Inverse Lighting Design for Interior Buildings Integrating Natural and Artificial Sources

Eduardo Fernández[a], Gonzalo Besuievsky[b]

[a]*Centro de Cálculo, Universidad de la República, Uruguay*
[b]*Geometry and Graphics Group, Universitat de Girona, Spain*

Abstract

In this paper we propose a new method for solving inverse lighting design problems that can include diverse sources such as diffuse roof skylights or artificial light sources. Given a user specification of illumination requirements, our approach provides optimal light source positions as well as optimal shapes for skylight installations in interior architectural models. The well known huge computational effort that involves searching for an optimal solution is tackled by combining two concepts: exploiting the scene coherence to compute global illumination and using a metaheuristic technique for optimization.

Results and analysis show that our method provides both fast and accurate results, making it suitable for lighting design in indoor environments while supporting interactive visualization of global illumination.

Keywords: Lighting Design, Inverse Problem, Global Illumination

1. Introduction

Lighting design is an important issue for sustainable buildings which involves both setting natural and artificial lights as well as meeting energy distribution goals. This process requires accurate lighting simulations, which are known to be computationally expensive for a single model and may become prohibitive when directly exploring lighting configurations for several sources. An efficient alternative to this computational task is to use an inverse lighting method. Inverse lighting designates all setting in which, unlike traditional direct calculations, illumination aspects are unknown and must be determined. If we know in advance the desired illumination at some surfaces, an inverse lighting approach can establish the missing parameters (e.g. light position, shape, and power emission, among others).

Providing computationally efficient inverse lighting tools is a challenge. The whole process involves two complex computational tasks: the global illumination simulation and the search for an optimal solution. The first task is crucial for accurate lighting design. Computing the indirect illumination constitutes a simulation of the light transport process through multiple bounces around the environment, and requires dense numerical solutions. For the second task, an optimization process is used to find a solution that fulfills some requirements. The best solution that optimizes a given goal is chosen. The problem is difficult to compute because the solution search space is generally huge.

Inverse lighting is not a new research topic. Several approaches have been proposed based on different motivations, assumptions and optimization strategies. Some of the techniques already explored are genetic algorithms [1], inverse radiosity systems [2, 3] and heuristic methods [4]. Most of these works provide only numerical solutions for each specific kind of environment, showing that an acceptable solution is eventually found. In general, all of the techniques are time consuming (requiring minutes or even hours) and are not designed for an interactive design cycle. Another limitation is that no technique to date includes electric sources integrated with natural lighting, as found in real buildings (see Figure 1).

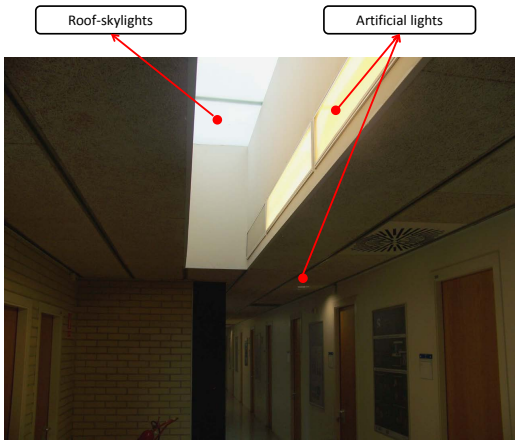

Figure 1: Artificial light sources integrated with skylights in a real building.

In this paper we present a novel inverse lighting method that efficiently shortens the execution time and integrates natural and artificial light sources. Given user illumination goals and a set of geometric restrictions and lighting intentions, our system provides optimal light source positions and optimal shapes for skylight installations in interior architectural models. The key element of our method is to exploit the coherence of architectural models to build a global illumination representation that allows designers to explore many solutions efficiently. This functionality is encoded into a low-rank radiosity representation, used as a solver called from an optimization method based

on the Variable Neighborhood Search (VNS) method [5].

The main contributions of our approach are as follows:

- We provide both a fast and accurate method for inverse lighting that allows designers to browse solutions in short design-cycle times.
- We provide a flexible lighting design approach in which light sources can be specified at any place in the environment.
- We provide a method that integrates artificial light sources with skylight sources.

The rest of the paper is organized as follows. The following section presents the related work. Section 3 provides an introduction to the problem definition. In section 4, the mathematical basis of the problem and of the proposed solution is developed. The main results of five inverse lighting experiments are exposed in section 5. The last section is devoted to the conclusions of this study and future work.

2. Related Work

There are two key areas of knowledge related to the inverse lighting problem: numerical optimization and global illumination. On the one hand the huge search space generated by inverse problems must be tackled by heuristic search-based techniques avoiding costly brute-force approaches. On the other hand, lighting simulation is required for each solution found in the search process. In this section we review the main related work on inverse lighting problems.

2.1. Inverse Lighting

Direct methods calculate data from a specific configuration of model parameters. In contrast, inverse problems generally infer the properties (or model parameters) of a physical system from observed or desired data. Inverse problems are usually numerically complex and are of interest in a wide range of fields in lighting engineering and lighting design.

One of the first attempts to infer emitter position and shape (parameters), given expressed lighting intentions (desired data), is presented by Schoeneman et al. [6]. These authors introduced the idea of providing an iterative numerical solution to achieve results from a "spray-painting" user-interface description. The interactivity was achieved only for direct illumination. Several works searching for similar goals but driven by different motivations and assumptions were later proposed. A survey of this topic was reported by Patow and Pueyo [7]. Contensin [3] formulated an inverse radiosity method based on a pseudo-inverse analysis of the radiosity matrix. Costa et al. [8] proposed an optimization engine to deal with complex light specifications. Kawai et al. [2] performed the optimization over the intensities and directions of a set of lights as well as surface reflectiveness to best convey the subjective impression of certain scene qualities (e.g., pleasantness or privacy), as expressed by users. Their so-called radioptimization system is a framework that determines optimal setting parameters based on unconstrained optimization techniques used in conjunction with a hierarchical radiosity solver [9]. Castro et al. [4] used heuristic search algorithms combined with linear programming to optimize light positioning with an energy-saving goal. Similar problems were solved with closely related techniques. Pellacini et al. [10] presented an interactive system for computer cinematography that allows users to paint the desired lighting effects in the scene, and a solver provides the corresponding parameters to achieve these effects using a non-linear optimization method. Gibson et al. [11] solve the inverse lighting problem through iteration of virtual light sources in the context of photometric reconstruction data.

Considerably less work has been devoted to optimizing daylight sources, such as openings and skylights. The problem of finding the modeling shapes for lighting goals is more complex for daylight sources than for artificial lights, because in the former case, we are dealing with a dynamic light source. An inverse method for designing opening buildings is presented by Tourre et al. [12] based on the evaluation of potential elements with relation to an interior lighting intention. In Besuievsky and Tourre [13], the method is extended for accurate sky computation with exterior occlusion. These approaches consider an anisotropic distribution of the light over the potential opening. Our system considers only openings with diffuse filters, such as typical skylight roof installations. However, our method greatly improves both accuracy and speed, also allowing interactive visualization results.

2.2. Coherence in Global Illumination

Independent of the strategy used to tackle the inverse lighting problems, the global illumination function must be evaluated many times prior to finding a converged solution. For this purpose an efficient method should be used to compute the solution for each setting of parameter values. However, research on this point has not been emphasized. The use of coherence is crucial to improve the global illumination computation in inverse lighting. Castro et al. [4] improved this known expensive computation by re-using random walk paths. They build and store, in a preprocessing step, an irradiance matrix that allows computing, for each patch of the scene the power contribution of several fixed light points. The main restrictions of this approach are that the authorized light positions must be predefined and that all of the light sources are point lights. In our work, we used a low-rank radiosity method (LRR) [14] that allows computers to solve the radiosity equation in real-time with infinite bounces for scenes with dynamic lighting and a relatively small computer storage. With this method no restrictions are required for the light sources: the sources could be anywhere in the scene and area light sources can be allowed, as well. Other approaches, such as the one presented by Kontkanen et al. [15], which uses wavelets to store a pre-computed matrix, could also be used for this purpose.

2.3. Optimization

An optimization problem consists of finding the best solution from all of the feasible solutions, which are defined through a

set of constraints. For illumination purposes, each constraint is related to a lighting intention for all or part of the scene. Although optimization is a well known topic, there is no computational algorithm that will always provide the global minimum for a general non-linear objective function. Finding the optimal solution by *brute force* is usually not feasible in a reasonable time because of the huge search space of the possible states. Heuristic algorithms avoid visiting the whole search space, by means of designing rules that drive the search towards optimal solutions. There are a large number of heuristic search algorithms in the literature, which can potentially be used to solve lighting problems. Hill climbing [16], beam search [17] and simulated annealing [18] are some of the most commonly used algorithms. Castro et al. [4] explored a wide range of these algorithms to solve optimal economical light positioning. In [19] and [20], the scenes are simplified to rectangular spaces, and the inverse problem is solved through a generalized extremal optimization approach. In our work, we used the VNS metaheuristic for optimization problems.We adapt this technique to our illumination problem and show that good optimization results can be achieved.

3. Problem Definition

The main goal of our proposal is to provide a helpful tool for efficient lighting design for both light sources and skylight installations. In this section we describe the lighting design problem formulation and our system proposal.

We consider diffuse environments, that is, all of the surfaces have perfectly diffuse materials with no specular component. Area light sources are also considered as Lambertian, with constant emission power. For roof-skylight sources we consider that a diffuse filter with a homogeneous transmittance coefficient is used. This system one of the most commonly used systems in real buildings. This system provides diffuse and controllable sunlight, which creates a desirable ambient light [21]. These kinds of skylights, because they scatter light homogenously, can also be considered as Lambertian emitters. However, the difference between these sources and artificial light sources is that the emission varies over time.

The energy goals are also driven in different ways: for artificial lights, we must aim for the most economical solution, whereas for skylights, in general, we aim to obtain as much light as possible, satisfying geometric restrictions. When designing daylight systems, it is beneficial to consider the solution across all sun positions (time of the day) and climatological conditions (sunny or cloudy). Although this variation is an important issue, for this work, we consider only the average of all of the incoming intensities. However, our mathematical framework can also take into account dynamic daylight changes. A further development of this subject is left for future work.

To specify the design task and find the optimal solution given a 3D interior space to illuminate, first, we must define the variables involved in the optimization, the constraints to satisfy, and the optimization goals.

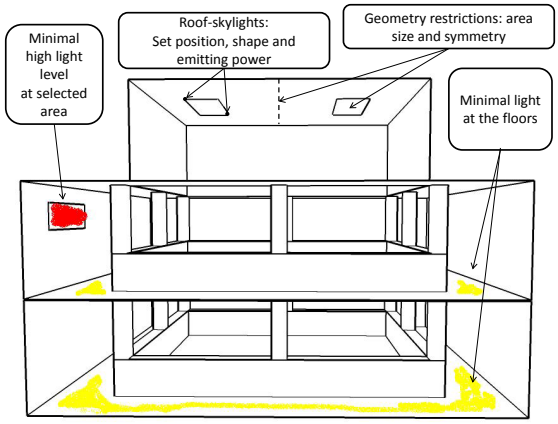

Figure 2: An example sketch of a design configuration. Skylights with area and symmetry restrictions must be installed in the roof, with the goal of achieving as much light as possible in the scene. Some special places in the wall require a minimum intensity. If a light source is required to achieve all of the restrictions, the system computes the optimal position and emissive power.

3.1. Optimization Variables

In the lighting design problem, the optimization variable is generally related to the light source specification. The light sources are no longer fixed as in a direct simulation, and optimal parameter values must be found for the emission, position, and shape. In our case, we consider rectangular area light sources with these three variables for optimization (see Figure 2).

3.2. Constraints

Constraints are the restrictions, whether imposed by the light designer or due to constructive building reasons, that must be satisfied in the illumination problem. Two different categories of constraints are considered: geometric restrictions and lighting intentions. For the first category, we consider any imposed restriction that the light source must achieve (such as light size, aspect ratio, in-between distances of sources or symmetries). For example, building constructive constraints regarding the installation of skylight sources in a roof may impose a regular distance between the skylights as well as that they must be aligned along a given axis. For lighting intentions, we consider those constraints that must be satisfied at the surfaces. Intentions are described by inequality constraints that specify the interval of light intensity that each surface is allowed to reflect.

3.3. Optimization Goals

Our goal is driven by the intention of optimizing energy consumption. Thus, we used the minimization of energy use as an objective function to select the best solutions among the many possible ones. In general, in a lighting-optimization problem such as the one we are describing, there may be an infinite number of possible solutions. We associate energy optimization for our lighting problem in the following way:

- For artificial light sources we will search for the most economical solution, that is, the one that minimizes the power consumption.
- For skylights, where light comes from natural resources, we aim to find the maximal global light-power solution. This way, less artificial light may be needed in the environment.

The pipeline design of our approach is described in Figure 3. Given an architectural interior model for lighting design, in which reflectance surfaces are already defined, the user first configures the parameters to find the optimal solution. These parameters specify where to put the light sources as well as the variables to optimize (source position, size and emission), the geometric restrictions and the lighting intention to achieve, and the energy goals to optimize. Before the optimization process begins, we first pre-process the scene to obtain a compact representation of the form-factor matrix of the elements of the scene. For this purpose, we use a low-rank radiosity method. The optimization method works by getting the compact representation found and a design configuration, to obtain a fast result that can be visualized interactively. Regarding the resulting values, the designer can modify the setting parameters to search for a new solution.

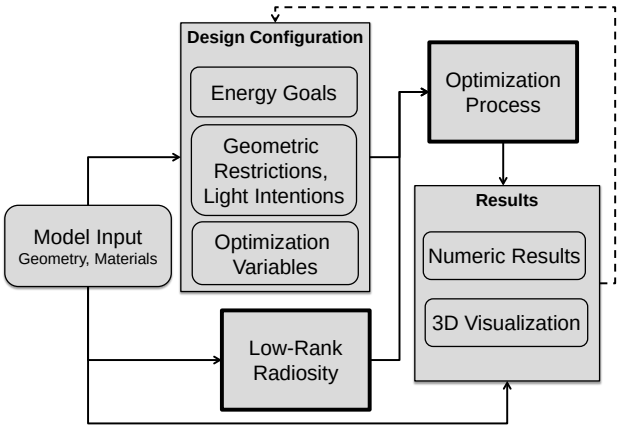

Figure 3: Pipeline system.

4. Mathematic Foundation

Our solution proposal is based on a two-step approach. In this section we describe details of both steps.

4.1. Problem Formulation

We explain here how to model the optimization problem as an unconstrained problem. Further development of this topic is reported by Kawai et al. [2] and Luenberger and Ye [22].

The goal of the problem can be formulated as the optimization of a function $f(x)$ that usually represents the power emitted by the artificial light sources or the total light power of the scene. There are also constraints related with geometric restrictions and lighting intentions. The general formulation of the optimization problem is expressed in Equation 1 where S is the set of feasible values for x.

$$\begin{aligned} &\text{minimize } f(x) \\ &\text{subject to } x \in S \end{aligned} \tag{1}$$

S can be formulated as a set of functional constraints, $S = \{x : c_i(x) \leq 0, i = 1 \cdots p\}$, where each $c_i(x) \leq 0$ is an inequation that defines a constraint, and p is the number of constraints. This set can be transformed into a continuous penalty function $P(x)$, which "turns on" when a constraint is not satisfied, i.e. $P(x) = 0$ when $x \in S$, and $P(x) > 0$ when $x \notin S$. The main idea behind the penalty method is the conversion of a constrained problem (Equation 1) into an unconstrained problem of the form:

$$\text{minimize } f(x) + P(x) \tag{2}$$

The penalty function used in this work has the form expressed in Equation 3, where *pow* is an even positive integer and W_i is a positive weight associated with each constraint.

$$P(x) = \sum_{i=1}^{p} \{W_i \times (\max[0, c_i(x)])^{pow}\} \tag{3}$$

The weights W_i must be adjusted to ensure that the solution of Equation 2 will approach the feasible region S.

In lighting design problems, the evaluation of the optimization goal $f(x)$ and some constraints (which we call $c_i^{Rad}(x)$) requires a radiosity evaluation of the scene. However, there are other constraints that do not depend on radiosity values ($c_i^{NoRad}(x)$), such as constraints that control the shape and location of the light sources. To avoid unnecessary radiosity evaluations, it must first be checked that $c_i^{NoRad}(x) \leq 0, \forall i$. So, the optimization problem expressed in Equation 2 can now be formulated as shown in Equation 4, where $P^{Rad}(x)$ is a penalty function that includes only the $c_i^{Rad}(x)$ constraints.

$$\begin{aligned} &\text{minimize } f(x) + P^{Rad}(x), \\ &\text{subject to } \{c_i^{NoRad}(x) \leq 0\} \end{aligned} \tag{4}$$

4.2. Low-Rank Radiosity

In this section we present a method to efficiently assess the radiosity equation, which is used to solve the optimization problem.

In the discrete radiosity problem, the radiosity of the scene is computed by solving the linear system shown in Equation 5.

$$(\mathbf{I} - \mathbf{RF})B = E \tag{5}$$

In this equation, $\mathbf{I}$ is the identity matrix with dimension $n \times n$ (n is the number of patches), $\mathbf{R}$ is a diagonal matrix that stores the reflectivity of the patches, $\mathbf{F}$ is the matrix with the form factors F_{ij} (which indicate the fraction of light reflected by the patch i that arrives to the patch j), B is a vector with the radiosity value of each patch, and E is the emission vector of the scene.

It is very likely that the (**RF**) matrix of Equation 5 has a low numeric rank because each row $(\mathbf{RF})_i$ is computed based on the scene view from the same element i. As most close pairs of patches have a very similar view of the scene (see Figure 4), (**RF**) has many similar rows resulting in a reduction of the numerical rank. The rank reduction of (**RF**) matrices allows for the matrices to be approximated by the product of two matrices $\mathbf{U}_k\mathbf{V}_k^T$, both with dimension $n{\times}k$ ($n{\gg}k$), without losing relevant information about the scene.

4.2.1. Low-Rank Approximation

The product $\mathbf{U}_k\mathbf{V}_k^T$ generates a matrix with dimensions $n{\times}n$ and rank k. The memory requirement of $\mathbf{U}_k$ and $\mathbf{V}_k^T$ is $O(nk)$, significantly less than $O(n^2)$ that would be required to store the matrix (**RF**). This reduction is especially appreciated when $n{\gg}k$, due to the spatial coherence of the scene. In this way, the memory saving allows for the information to be stored in the main processor memory, facilitating work with large scenes.

Replacing (**RF**) by the low-rank approximation $\mathbf{U}_k\mathbf{V}_k^T$ in Equation 5 allows us to obtain the row-rank radiosity (LRR) equation 6. The unknown is no longer B but rather an approximation $\widetilde{B}$ of the radiosity.

$$\left(\mathbf{I} - \mathbf{U}_k\mathbf{V}_k^T\right)\widetilde{B} = E \tag{6}$$

The matrix $\left(\mathbf{I} - \mathbf{U}_k\mathbf{V}_k^T\right)$ is now invertible using the Sherman-Morrison-Woodbury formula [23].

$$\widetilde{B} = E + \mathbf{U}_k\left(\left(\mathbf{I}_k - \mathbf{V}_k^T\mathbf{U}_k\right)^{-1}\left(\mathbf{V}_k^T E\right)\right) \tag{7}$$

To find $\widetilde{B}$ using Equation 7, $O(nk^2)$ operations and $O(nk)$ memory are required. For scenes with static geometry and dynamic lighting (i.e., only the independent term E varies in Equations 5 to 7), part of the computational effort can be pre-computed and stored. Equation 7 is now written as follows:

$$\widetilde{B} = E - \mathbf{Y}_k\left(\mathbf{V}_k^T E\right), \tag{8}$$

$$\text{where } \mathbf{Y}_k = -\mathbf{U}_k\left(\mathbf{I}_k - \mathbf{V}_k^T\mathbf{U}_k\right)^{-1}$$

where $\mathbf{Y}_k$ is a $n{\times}k$ matrix that is computed once (as well as $\mathbf{U}_k$ and $\mathbf{V}_k$). After $\mathbf{Y}_k$ is found, the radiosity calculation has complexity $O(nk)$. This result is very useful to develop a new methodology for inverse lighting problems with static geometry [14]. Fernández et al. [24] combined Equation 8 with GPU architectures to solve the radiosity problem in real time, hundreds of times per second in scenes with tens of thousands of elements.

Another important result is that the LRR methodology is a direct method. Equation 8 can also be formulated as $\widetilde{B} = \mathbf{G}E$, so the matrix $\mathbf{G}{=}\mathbf{I}{-}\mathbf{Y}_k\mathbf{V}_k^T$ is a global operator that manages the infinite bounces of light in a single operation. The matrix $\mathbf{G}$ allows finding the radiosity values for any set of p patches ($p < n$) without solving the radiosity for all of the patches (as in iterative methodologies like hierarchical radiosity [25]). Only p rows of $\mathbf{G}$ are needed to find the radiosity values (i.e. $\mathbf{G}_p{=}\,\mathbf{I}_p{-}\mathbf{Y}_{k,p}\mathbf{V}_k^T$, where $\mathbf{Y}_{k,p}$ consists of p rows of $\mathbf{Y}_k$ related to

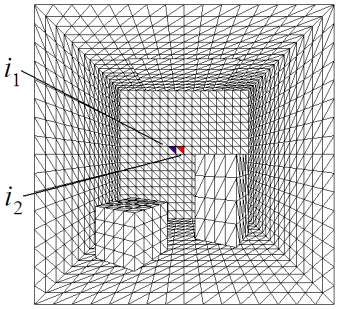

(a) Two close patches i_1 and i_2.

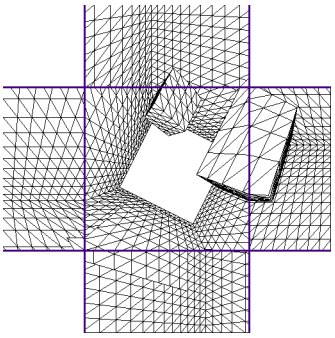

(b) Hemicube view from i_1.

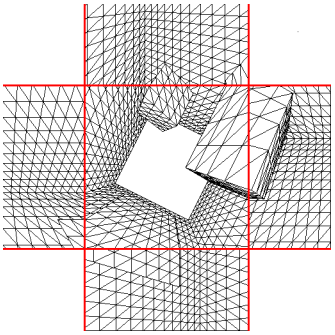

(c) Hemicube view from i_2.

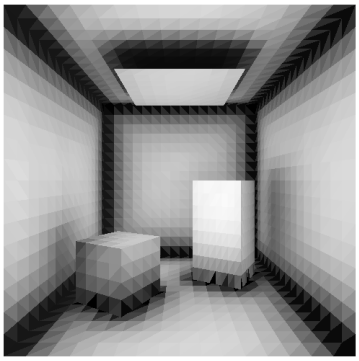

(d) Spatial coherence in the scene.

Figure 4: Close patches present similar views of the scene and generate similar rows in (**RF**) (see [14]). In (d), the coherence of each patch is measured (a darker color indicates lower coherence).

the p patches, and the same also applies to $\mathbf{I}_p$). Therefore, the radiosity calculation goes down to $O(n + pk)$ operations.

Using the LRR methodology, the global operator **G** is computed while avoiding the iterative utilization of Neumann series, as is employed by Kontkanen et al. [15] and Lehtinen et al. [26], taking advantage of the fact that (**RF**) is a low-rank matrix.

4.2.2. Direct Radiosity Method in Inverse Lighting Problems

Any optimization algorithm used to solve inverse lighting problems finds thousands of feasible solutions, to identify one that meets all of the constraints and optimizes the objective function. For most of the optimization time, the algorithm is focused on the radiosity calculation; consequently, the speed of the optimization algorithm is mainly related to the speed of the radiosity solver. Our proposal is based on the use of the LRR method as a fast and direct solver.

Besides solving the radiosity method faster when only the radiosity of p patches are needed, the LRR method also can be used to speed up the optimization process of complete scenes with good spatial coherence. Because close patches have similar radiosity properties, the radiosity values of a representative set of patches provide enough scene information for optimization purposes.

Following this approach, an optimal solution found using a subset of patches could be the starting point of another optimization process with a greater set of patches. After the execution of several optimization processes, using an increasing sequence of sets of patches, this multilevel strategy could terminate after considering all of the scene patches. Given the right conditions, it is expected that a multilevel strategy like this wouldl converge much faster than only one optimization process with all of the patches.

4.3. Heuristic Search and Optimization

We developed an algorithm to solve the inverse lighting problem based on the VNS metaheuristic [5]. This methodology is based on the idea of successive explorations of a set of neighborhoods $(N_1(x), N_2(x), \cdots, N_k(x))$. The method explores, either at random or systematically, a set of neighborhoods to obtain different local optima. Each neighborhood has its own local optimum, and it is expected that the global optimum is the same as a local optimum for a given neighborhood (see Figure 5).

The set of neighborhoods is usually nested (i.e. $N_1(x) \subset N_2(x) \subset \cdots \subset N_k(x)$). This strategy will be effective if the different neighborhoods used are complementary in the sense that a local optimum for a neighborhood N_i will not be a local optimum in the neighborhood N_j (when $N_i \subset N_j$).

We used the general pseudocode of the VNS strategy to develop an algorithm for our lighting problem (see Algorithm 1). The algorithm attempts to find x such that the function $f(x) + P^{Rad}(x)$ is minimized, and that all of the $c_i^{NoRad}(x) \leq 0$ constraints are satisfied.

In our implementation, each neighborhood N_k has two parameters, v and r, that define the neighborhood's scope. The parameter v establishes the number of optimization variables

Algorithm 1: Radiosity VNS.

Input: Set of neighborhood structures N_k for $k = 1, ..., k_{max}$
Output: The most optimal solution found
$x = x_0$; `/* Generate the initial solution */`
while not *Stopping Criteria* **do**
  $k = 1$;
  while $k <= k_{max}$ **do**
    Find a better neighbor x' of x in $N_k(x)$ by local-search;
    if $\exists\ x' | \{f(x') + P^{Rad}(x') < f(x) + P^{Rad}(x)\}$
    and $(c_i^{NoRad}(x') \leq 0\ \forall i)$ **then**
      $x = x'$;
      $k = 1$;
    end
    otherwise
      $k = k + 1$;
    endsw
  end
end

that are modified at the same time, and r defines a normalized interval of variation. For instance, $v = 1$ and $r = 0.1$ means that, in each trial of the local search, a variable x_i of x is randomly selected, and the variable's value is substituted by another value chosen from the interval $x_i \pm 0.1$. In one step, a variable related to the position of the light is modified; in the next step, the power of the light emission is modified; and so on. Following the parametric neighborhood definition, a grid of neighborhoods can be defined, considering all of the combinations of values $v = 1, 2, \cdots, nvar$, $r = 0.1, 0.2, \cdots, 1$. Then, the set of neighborhoods used by the algorithm is a selectionand eventually allof the neighborhoods defined in the grid.

Using the problem formulation expressed in Equation 4, the local-search algorithm first controls that each tested neighbor x' fulfills $c_i^{NoRad}(x') \leq 0\ \forall i$, before the radiosity is evaluated and the value of the goal (i.e. $f(x) + P^{(Rad)}(x)$) is checked. This prior control avoids unnecessary radiosity calculations.

Different stopping criteria can be used, such as the time required to obtain a given target solution, the distance to the target solution or the number of iterations.

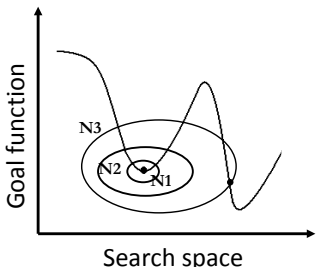

Figure 5: Variable neighborhood search using three neighborhoods (N1, N2 and N3). When a local optimum is found (as in N3), the search methodology continues at this point.

4.3.1. Multiobjective Optimization Problem

Many inverse lighting problems can be defined as an optimization problem with multiple objectives, such as the minimization of artificial power consumption and maximization of natural light influence. The mathematical definition of a multi-objective optimization problem (MOP) can be stated as follows:

$$\begin{aligned} \text{minimize } F(x) &= (f_1(x), f_2(x), \cdots, f_n(x)) \\ \text{subject to } x &\in S \end{aligned} \tag{9}$$

Multi-objective optimization problems and techniques are analyzed by Deb [27] and in Coello et al. [28]. The optimal solution for MOP is not a single solution as for mono-objective optimization problems, but a set of "non-dominated" solutions, that is, solutions for which it is not possible to improve one objective without impairing at least one other objective. This set of optimal solutions is called a Pareto front.

Many methodologies used to solve multi-objective optimization problems are founded on population-based metaheuristics, such as evolutionary algorithms [27, 28]. Other methodologies are based on scalar approaches [29], which transform a multi-objective optimization problem into a set of mono-objective problems. This approach allows using a single solution based on metaheuristics as the VNS. In our work, we implemented the ϵ-constraint method as a scalar approach. The ϵ-constraint method consists of optimizing one selected objective f_k subject to constraints on the other objectives $f_j, j \in [1 \cdots n], j \neq k$ of a MOP (see Equation 10). Hence, some objectives are transformed into constraints.

$$\begin{aligned} &\text{minimize } f_k(x) \\ &\text{subject to } x \in S \\ &f_j(x) \leq \epsilon_j, j = 1 \cdots n, j \neq k \end{aligned} \tag{10}$$

In this equation, each ϵ_j is an upper bound for the objectives. The ϵ-constraint method is run many times, changing the values of ϵ_j. This method generates a set of non-dominated solutions with good diversity properties. It is necessary to know a priori the suitable interval for each ϵ_j value.

5. Analysis and Results

To evaluate the fundamental aspects of our method, we built a set of five different experiments. The goal of the first experiment is to evaluate the convergence properties of the proposed algorithm. For this reason, a scenario is built in which the method must converge to a known solution. In another experiment, we check how the spatial coherence of the radiosity solution can help to decrease the convergence time. Next, we test how the algorithm addresses the fulfillment of the constraints (geometric restrictions and lighting intentions). Finally, the scenario of problems with multiple solutions is considered for two cases: a single objective problem with many practical solutions and a MOP study case. These experiments were designed to demonstrate the good properties of the method and to identify further areas for development.

For the daylight intensity, we used average data, not taking into account the date and time of the day or the variation of light intensity throughout the day. Thus, we present tests scenes as architectural prototype models, and we will develop adjustments for real data in future work.

All of the simulations were performed in a Matlab environment on a notebook computer (Intel Core i7-2670QM 2.2 Ghz processor with Turbo Boost up to 3.1 Ghz and 4 GB DDR3 memory).

5.1. 1st Experiment: Convergence

Scene : Patio building. Size (n×k): 24128×1508. The precomputation of $\mathbf{Y}_k$ and $\mathbf{V}_k$ takes about 12 minutes.

Goal : Find the shape and position of two area light sources such that the reflected radiosity $C(E)$ for emission E is close to a desired reflected radiosity C_{obj}.
$C(E) = B - E = -\mathbf{Y}_k \mathbf{V}_k^T E$
$C_{obj} = B_{obj} - E_{obj} = -\mathbf{Y}_k \mathbf{V}_k^T E_{obj}$.

Number of constraints : 8
The light emitters must lie in the ceiling.

Variables : 8
Four 2D coordinates that delimit the location of the light sources.

In this experiment, we test the capability of our method to approximate the initial conditions of the scene from a previously known radiosity solution. To build a known solution, we first choose two rectangular light sources at the ceiling of the patio (Figure 6a), which define E_{obj}. Then, the diffuse reflection of the scene C_{obj} is computed using the LRR method.(Figure 6b).

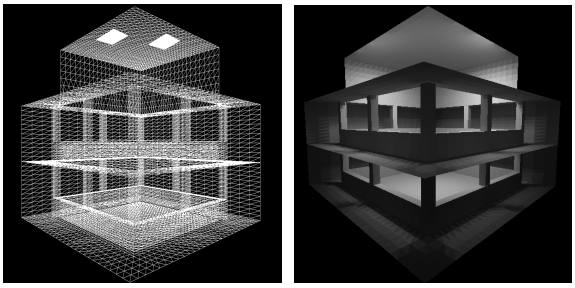

(a) Two emitters in the ceiling. (b) Reflected radiosity in patio.

Figure 6: Patio scene.

The algorithm attempts to find the location of two rectangular emitters E in the ceiling, such that the resulting radiosity reflected $C(E)$ minimizes the normalized Euclidean distance (Equation 11).

$$\min_E e(E) = \frac{\|C(E) - C_{obj}\|_2}{\|C_{obj}\|_2} \tag{11}$$

The space of possible solutions is composed of the set of lists of four roof patches that define the diagonal extremes of two skylights. In this example, the roof is composed of 1024 quads, and therefore, the possible solutions can be estimated as $C_4^{1024}/4 \approx 11.4 \times 10^9$ (the division by 4 is due to symmetry

considerations). A brute-force exploration of all of the solution space is not feasible on desktop computers.

There is a biunivocal relation between the radiosity (B or C) and the emission (E) caused by the existing linear relations expressed in Equations 5 and 6. If the goal of the problem is to find C close to C_{obj} (and the problem is not ill-conditioned), then E is usually close to E_{obj}. Figure 7 shows different runs of the VNS algorithm. Each image is a 2D projection of the ceiling, where E_{obj} is presented in green, and E is presented in red. The leftmost column shows the starting configuration for each run, and the rightmost column shows the final result. The center columns show the intermediate results.

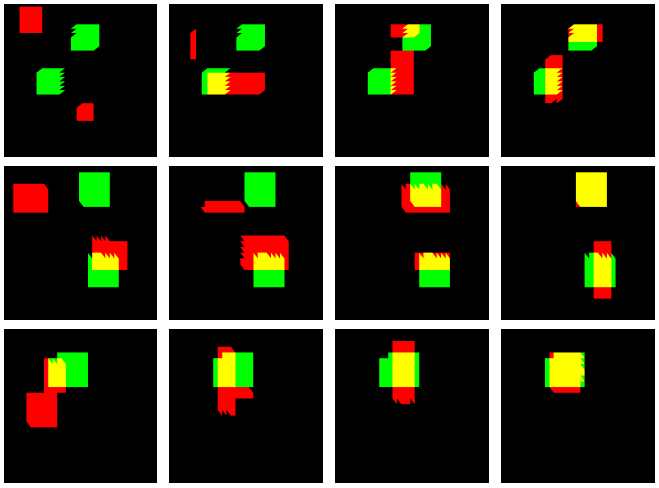

Figure 7: Visualization of the emitters in the ceiling in three runs of experiment 1. Each row is a different run (from left to right). In each run, E (in red) is approaching to E_{obj} (in green).

Figure 8 shows, from top to bottom, another view of a VNS run (the first row of Figure 7). The left column presents the convergence of the reflected radiosity $C(E)$ to the desired radiosity C_{obj} (Figure 6 (b)). The right column displays the radiosity errors of each $C(E)$ found. Those patches coloured green comply with C_{obj}>$C(E)$, and those colored red satisfy that C_{obj}<$C(E)$. The gray patches meet C_{obj}≈$C(E)$.

5.2. 2^{nd} *Experiment: A Multilevel Method*

Considering that the patio scene has good spatial coherence, it can be assumed that the distance $e_p(E)$ is a good approximation of $e(E)$ (Equation 12), where p is the number of representative patches, $C_p(E) = -\mathbf{Y}_{k,p}\mathbf{V}_k^T E$, and $C_{p,obj} = -\mathbf{Y}_{k,p}\mathbf{V}_k^T E_{obj}$.

$$\min_E e_p(E) = \frac{\|C_p(E) - C_{p,obj}\|_2}{\|C_{p,obj}\|_2} \tag{12}$$

For the patio scene, 50000 radiosity evaluations $C(E)$ take approximately 100 minutes ($O(nk)$), and the computation of $e_p(E)$ with p=$n/16$, takes only 11 minutes ($O(n + pk)$).

Given the above results, two sets of experiments were conducted to demonstrate the potential of using spatial coherence properties. In the first experiment, the stop condition of the VNS algorithm is set to $e_p(E_i)$<0.03, with p=$n/16$. After the algorithm stops, the real distance $e(E)$ is calculated. A total of 30 runs were conducted to allow for a statistical comparison between both of the distances. The statistical analyses reveal that the ratio $r(E_i)$=$e(E_i)/e_p(E_i)$ has a mean μ=1.24 and a standard deviation σ=0.29. Assuming that r has a normal distribution, then $\mu\pm2\sigma$ is the 95.5% confidence interval. Therefore, it can be concluded that, if $e_p(E)$<0.03, then $e(E)$<0.03(μ+2σ)= 0.03(1.24+2 · 0.29)=0.055 with a probability of 95.5%.

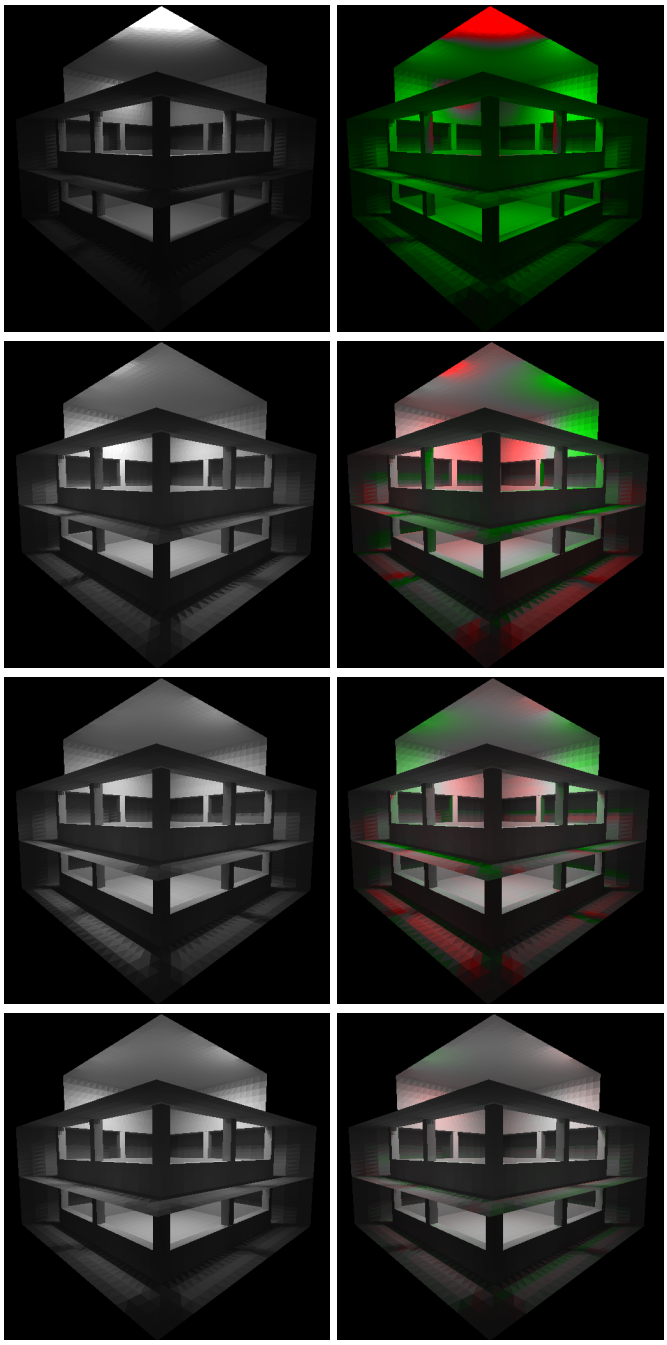

Figure 8: Each row correspond to a stage in the optimization process (top-to-bottom). Left: the reflected radiosities ($C(E)$). Right: The colors show the difference between $C(E)$ and C_{obj}. Green means C_{obj}>$C(E)$, and red means C_{obj}<$C(E)$.

Figure 9 shows the convergence path for five runs of the algorithm, each with a different starting seed. The values of the objective function are shown in blue. The stop conditions of the algorithm are a distance threshold ($e_p(E_i) < 0.03$; the red dotted line in Figure 9) and the number of radiosity evaluations (50000). For this scene, because the threshold is reached after an average of 26000 radiosity evaluations, we can conclude that the algorithm took, on average, 340 seconds to reach the solution.

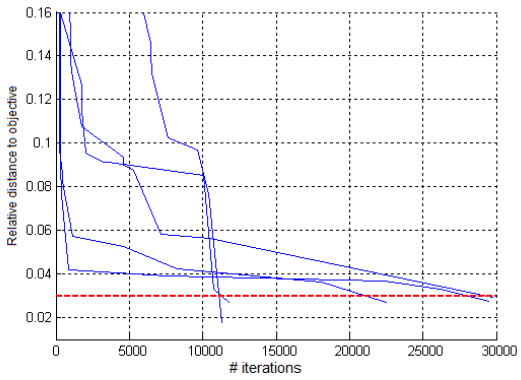

Figure 9: Convergence of VNS algorithm for different runs.

The above results motivate a second set of experiments consisting of the implementation of a multilevel method with the aim of accelerating the optimization process. The multilevel algorithm used consists of three consecutive optimization processes, where each process is related to a greater set of patches. In addition to all of the scene patches, we also consider two subsets of scene patches with $p = n/16$ and $p = n/64$ elements. First, we solve the optimization problem with the smallest set of patches ($p = n/64$). The solution found becomes the starting point for a second run of the optimization algorithm, this time with a mid-size set of patches ($p = n/16$). Finally, a last run is performed that includes all of the scene patches.

Comparing the result previously obtained with all the scene patches (100 minutes), we now take only 470 seconds for the same total number of radiosity evaluations and same quality results. Because each optimization algorithm stops when e_p is lower than a certain threshold, the statistical results for the patio scene show that the sequence of optimization problems stops after a mean of 28500 iterations and 310 seconds. Figure 10 shows a sequence of three consecutive runs of the algorithm, following the above scheme. In this example, a solution that considers all of the patches is found in 350 seconds. A new processing run starts when the previous run has an error e_p lower than 0.03.

5.3. 3rd Experiment: Many Constraints

Scene : Patio building. Size ($n \times k$): 24128×1508.

Goal : Maximize the light power in the scene: max $\sum_{\forall i} C_i A_i$.

Constraints :

- One rectangular light source in the ceiling.

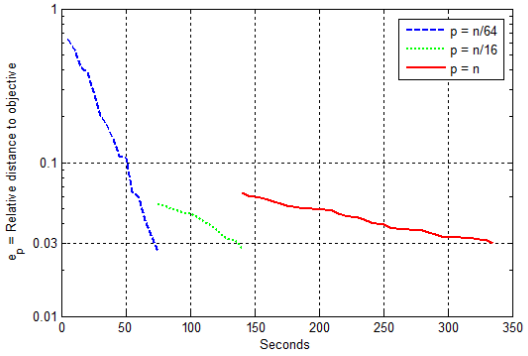

Figure 10: Convergence of VNS algorithm (multilevel method).

- Reflected Radiosity $\forall i$: $C_{min} \leq C_i \leq C_{max}$.
- Bounded area: $A_{min} \leq$ Area of skylight $\leq A_{max}$.

Variables : 4

Two 2D coordinates that define the light shape and position.

This experiment studies the convergence of the VNS algorithm in maximizing the total power reflected from the scene ($\max \sum_{\forall i} C_i A_i$), where C_i and A_i are the radiosity reflected and the area of patch i, respectively. A rectangular skylight must be installed in the ceiling. As explicit constraints, the radiosity value of each patch and the area value of the skylight should be placed within defined ranges.

Figure 11 shows the evolution of the algorithm. The red dotted line shows the value of the penalty function $P^{Rad}(x)$ in each iteration. As explained in Section 4, when all of the constraints are fulfilled, the penalty function value is 0. The continuous blue line shows the total light power reflected by the scene.

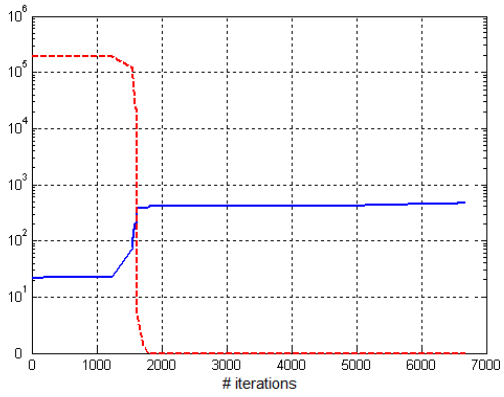

Figure 11: Convergence to feasible solutions.

Figure 12 shows the evolution of the same problem when a constraint is modified. Now $C_{min} \leq C_i \leq C_{max}/4, \forall i$. Given this configuration of constraints, there is no feasible solution set, and, as shown in the plot, the algorithm also fails to find a feasible solution. Therefore, the designer must change one or more constraints to find a solution that meets all of them.

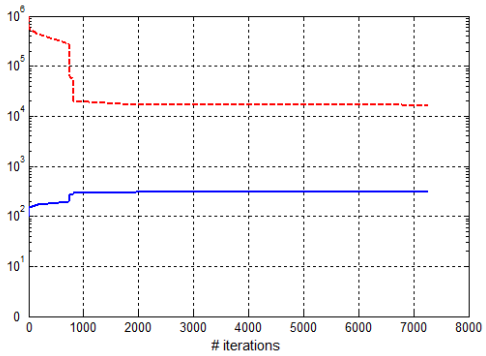

Figure 12: Unfeasible convergence.

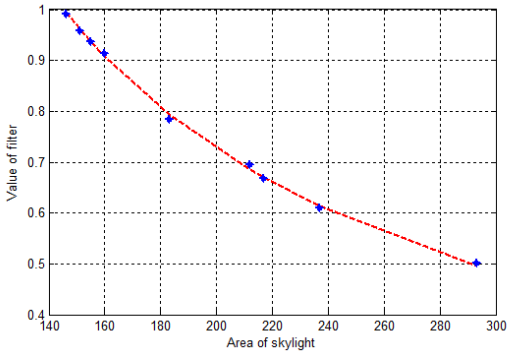

Figure 13: Relation between skylight area and the filter value.

It is important to determine whether the constraints pursued are possible to fulfill. As shown in the pipeline system (Figure 3), the analysis of the results after the optimization process can be used to redefine the specification of the problem with new lighting intentions.

5.4. 4^{th} *Experiment: Many Solutions*

Scene : Patio building. Size (n×k): 24128×1508.

Goal : Maximize the light power in the scene: max $\sum_{\forall i} C_i A_i$

Constraints :

- One rectangular light source in the ceiling.
- Reflected Radiosity $\forall i$: $C_{min} \leq C_i \leq C_{max}$.
- Bounded area: $A_{min} \leq$ Area of skylight $\leq A_{max}$.
- Filter value $0 \leq f \leq 1$.

Variables : 5

- Two 2D coordinates that define the light shape and position.
- A variable that defines the filter value.

This experiment is similar to the previous one, with an added filter value f to control the skylight emittance (f×e_{max}, where e_{max} is the maximum skylight emittance).

Each run of the algorithm converges to a different solution. In Figure 13, the blue asterisks show the pairs of skylight area and filter values found for several runs. The red dotted line shows a hyperbolic curve that almost fits the solutions.

The total light power produced by the skylight is almost the same in all of the solutions (skylight-area×filter is almost constant), which intuitively means that the smaller the area of the skylight, the more light must pass through the filter. In this case, the designer must identify the best solution from the set of optimal solutions provided by the algorithm.

5.5. 5^{th} *Experiment: A Case Study with MOP*

First problem:

Scene : Corridor. Size(n×k): 16736×1046. The pre-computation of $\mathbf{Y}_k$ and $\mathbf{V}_k$ takes about 8 minutes.

Goal : Maximize the natural light power: max $\sum_{\forall i} C_i A_i$

Constraints :

- Skylights delimited into areas S_1, S_2 and S_3.
- Skylights in S_1 and S_3 must be symmetric.
- The skylight in S_2 must be centered.
- Area of the skylights $\leq A_{max}$.
- Aspect ratio of the skylights ≤ 4.
- Radiosity reflected by the panels $\geq B_{min}$.

Variables : 6

- Two 2D coordinates that defines in S_1 the skylight shape and position of the skylight (the skylight in S_3 is symmetric).
- One 2D coordinate that delimits the position of the skylight in S_2 (centered skylight).

After 10^5 iterations it was not possible to find a feasible solution. The amount of natural light passing through the skylights does not fulfill the constraint for the panels. The designer may relax some of the constraints (i.e., increasing the area of skylights or decreasing the radiosity in the panels) to find feasible solutions. Another course of action would be the addition of small artificial lights near each panel to satisfy all of the predefined constraints (Figure 14). In this case, the problem is transformed into a MOP because the minimization of the artificial light power must also be considered.

Second problem (MOP):

Goal 1 : Maximize the light power in the scene: max $\sum_{\forall i} C_i A_i$

Goal 2 : Minimize the artificial light power: min $\sum_{\forall i} E_i A_i$

Constraints :

- The same set included in the first problem.

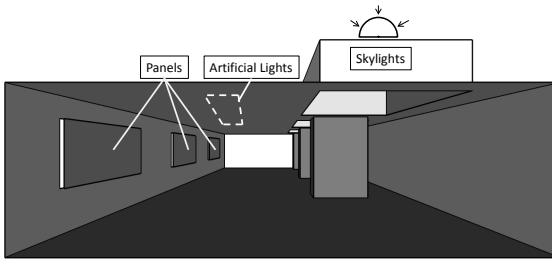

(a) Perspective view of the corridor scene.

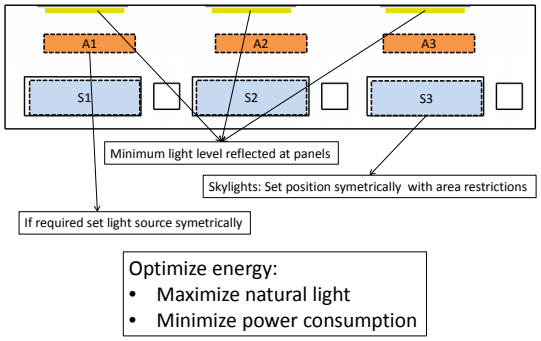

(b) Configuration scheme.

Figure 14: Corridor scene as a MOP.

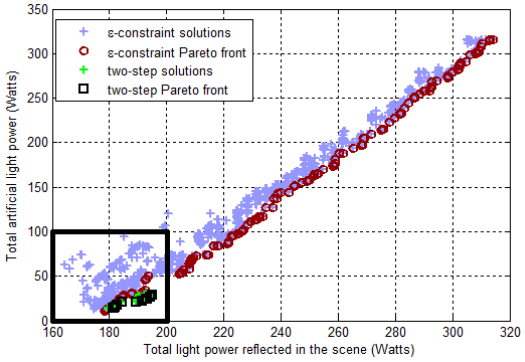

(a) General view of a set of feasible solutions.

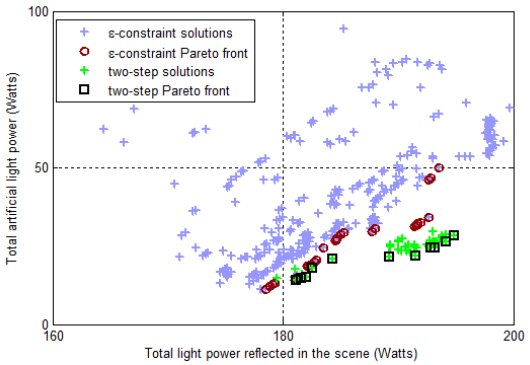

(b) Detail view of the area bounded in (a).

Figure 15: Feasible solutions found in a ϵ-constraint process (blue '+') and its corresponding Pareto front (red 'o'). Additionally, solutions found from a two-step process (green '+') and the associated Pareto front (black '□').

- Area light sources delimited into A_1, A_2 and A_3.
- Area light sources in A_1 and A_3 must be symmetric.
- The light area source in A_2 must be centered.
- Aspect ratio of each emitter ≤ 10.

Variables : 12

The same variables (6) used in the previous problem and 6 more related to the artificial light sources.

A multi-objective optimization process must be used to find a Pareto front of non-dominated solutions. In Figure 15, the blue '+' are a set of feasible solutions found when running the ϵ-constraint method, and the red '$\circ$' set is their associated Pareto front. The ϵ-constraint method minimizes the artificial light power (Goal 2) when all of the constraints are satisfied and when the total light power is greater than ϵ (a new constraint defined with Goal 1). The variable ϵ takes all of the even values between 170 and 260W, with 20000 radiosity evaluations each.

Besides the use of a method, such as the ϵ-constraint method, to find the Pareto front, another approach consists of solving the optimization problem using a procedure that follows the designer's intentions. For instance, if the designer wants to maximize the natural light that comes through the skylights, and the use of artificial light is only used to complete the illumination needed in the panels, then a good approach consists of a two-step process. First, an optimization problem is solved involving only the variables related to the skylights, ignoring all of the constraints associated with the panels and also ignoring all of the variables and constraints related to the artificial emitters. The goal of this problem is to maximize the total power of the natural light reflected in the scene (see Figure 16 (a)). In a second step, another optimization problem is solved, ignoring all of the variables and constraints related to the skylights, involving only the variables related with the artificial emitters and considering the panel's constraints. The goal of this problem is to minimize the light power of the artificial emitters (see Figure 16 (b)). In Figure 16 (c), it can be seen the position and shape of the skylights and emitters determined using the two-step process are shown.

Figure 15 shows the solutions found by the two-step process.The green '+' are the solutions found by this process, and the black '□' set is their corresponding Pareto front. The two-step process was executed 50 times, with 20000 iterations each.

Many of the 50 solutions found using the two-step method are better than (i.e., not dominated by) the ϵ-constraint Pareto front solutions, but the two-step method is concentrated in one extreme of the Pareto front. These results show that the Pareto front found contains rather good solutions and good diversity and also show that the two-step method is a very effective approach to find solutions that meet specific design goals.

Close Pareto front solutions can be caused by very different light source configurations. In Figure 15 (b), the two-step Pareto front is located in a narrow range of powers, and Experiment 4 shows that solutions with almost the same light power

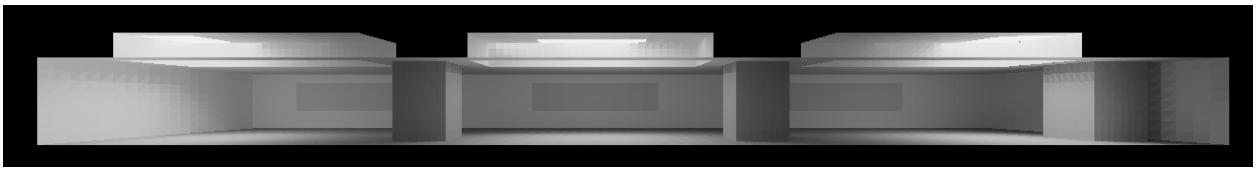

(a) Radiosity generated with optimized skylights (Goal 1, excluding panels constraints and artificial light sources).

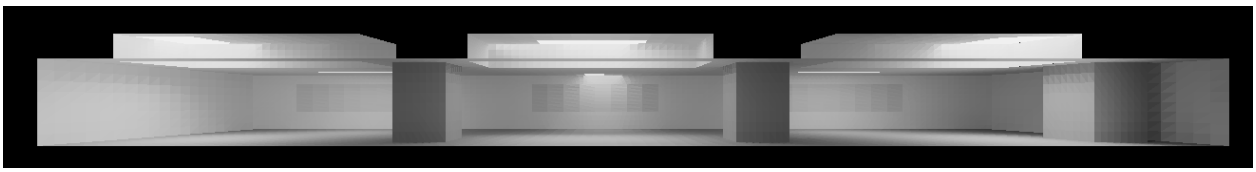

(b) Radiosity generated with optimized artificial light sources (Goal 2, including panels constraints and fixing the previous skylight solution).

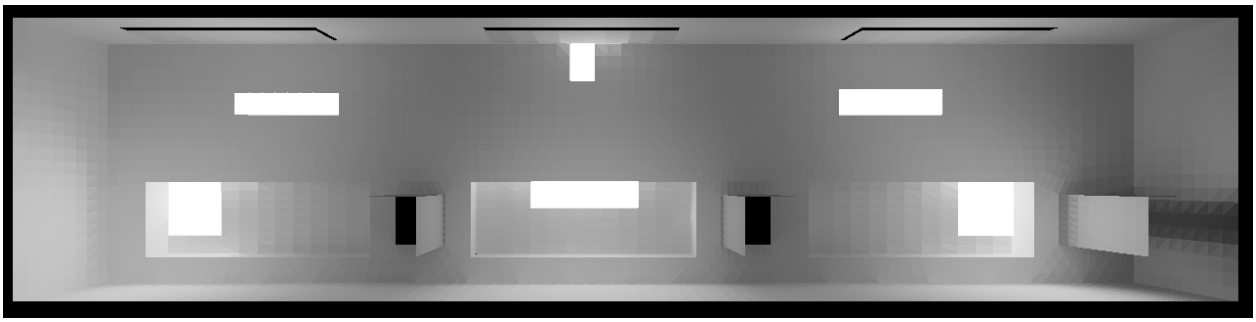

(c) Top view of the scene with the positioning solution of all of the area sources.

Figure 16: Solutions of the two-step optimization process for the corridor scene.

have different light-source configurations. Therefore, a designer must check all of the solutions to decide which one is the most convenient.

5.6. Summary Discussion

Numerically comparing our method with other previous inverse lighting techniques is a difficult task because each method provides different conditions. However, we can claim that we provide a fast solver for moderately complex environments with Lambertian surfaces. Using the acceleration technique described in our second experiment, we can obtain reliable results in only a few minutes, an improvement from recent works [4, 19]. Moreover, our system provides interactive radiosity visualization that can help in making design decisions.

The low-rank methodology, as a direct method, allows to find in $O(n + pk)$ the radiosity of p patches. This is faster than other iterative methods (like hierarchical radiosity) where the radiosity of all the scene must be solved, even if the algorithm optimizes the radiosity value of a single patch.

The low-rank methodology allows considering only diffuse scene surfaces, which is not true in many interior settings. To overcome this limitaion, a methodology based on radiance [15] used as a global illumination engine, could be analyzed and tested.

The reverse-engineering process applied for design, which computes the initial conditions for achieving a lighting effect, is not a simple issue. One important subject is the search for feasible solutions, where the methodology can provide sufficient assistance. Besides searching for a solution, our method also provides much more information about the range of possibilities that may occur when expressing a design intention. This information will allow for an interactive use of the design cycle, in which the designer can explore multiple possibilities. Further extending this concept, our system provides a MOP solver that finds a Pareto front of solutions. Given this set of optimal solutions, a designer must choose the ones that match his design ideas.

6. Conclusion and Future Work

We developed a novel technique of inverse lighting, combining the use of an optimization metaheuristic with the LRR technique as a radiosity solver. The paper addressed the problem of optimization with constraints, using the penalty method approach. A radiosity engine based on LRR methodology was used, taking into consideration the spatial coherence of the scene. Also, as LRR is a direct methodology, a multilevel scheme was tested, showing promising results. Finally, the case of MOP was analyzed, developing two methods based on VNS metaheuristic: ϵ-constraint, when the goal consists in finding a Pareto front, and the two-step optimization process, for the particular case when the goal is to maximize the natural light provided by skylights and minimize the power of artificial light.

Regarding future work, one objective consists in improving the technique using a CPU-GPU architecture in order to

speed up the VNS and LRR calculation times. Also it is necessary to explore the multilevel methodology deeper, to transform the basic scheme implemented into a more robust algorithm. In relation with the emitters, further work is needed to include anisotropic light sources and temporal and climate variation of the daylight sources. Another line of future work is the implementation of a MOP solver using a population-based metaheuristic like genetic algorithms. Following Talbi [29], this kind of metaheuristic allows a better diversification in the whole search space than single-solution based metaheuristic. Finally, the development of real examples and working experiences with designers are needed. This line of work will transform the code implemented into a design tool useful for architects and interior designers.

References

[1] Tena JE, Rudomin I. An interactive system for solving inverse illumination problems using genetic algorithms. In: Proceedings of Computacion Visual. 1997,.

[2] Kawai JK, Painter JS, Cohen MF. Radioptimization - goal based rendering. In: ACM SIGGRAPH 93. Anaheim, CA; 1993, p. 147–54.

[3] Contensin M. Inverse lighting problem in radiosity. Inverse Problems in Engineering 2002;10(2):131–52.

[4] Castro F, del Acebo E, Sbert M. Energy-saving light positioning using heuristic search. Engineering Applications of Artificial Intelligence 2012;25(3):566 –82.

[5] Hansen P, Mladenovic N. Variable neighborhood search: Principles and applications. European Journal of Operational Research 2001;130(3):449–67.

[6] Schoeneman C, Dorsey J, Smits B, Arvo J, Greenberg D. Painting with light. In: Proceedings of the 20th annual conference on Computer graphics and interactive techniques. ACM SIGGRAPH 93; New York, NY, USA: ACM; 1993, p. 143–6.

[7] Patow G, Pueyo X. A survey of inverse rendering problems. Computer Graphics Forum 2003;22(4):663–88.

[8] Costa AC, de Sousa AA, Ferreira FN. Lighting design: A goal based approach using optimisation. In: Lischinski D, Larson GW, editors. Rendering Techniques. Springer; 1999, p. 317–28.

[9] Hanrahan P, Salzman D. A rapid hierarchical radiosity algorithm. In: Computer Graphics. 1991, p. 197–206.

[10] Pellacini F, Battaglia F, Morley RK, Finkelstein A. Lighting with paint. ACM Trans Graph 2007;26(2).

[11] Gibson S, Howard T, Hubbold R. Flexible image-based photometric reconstruction using virtual light sources. Computer Graphics Forum 2001;20:203–14.

[12] Tourre V, Martin JY, Hégron G. An inverse daylighting model for caad. In: Proceedings of the 24th Spring Conference on Computer Graphics. SCCG '08; New York, NY, USA: ACM; 2008, p. 83–90.

[13] Besuievsky G, Tourre V. A daylight simulation method for inverse opening design in buildings. In: Rodríguez O, Serón F, Joan-Arinyo R, J. Madeiras J. Rodríguez EC, editors. Proceedings of the IV Iberoamerican Symposium in Computer Graphics. Sociedad Venezolana de Computación Gráfica; DJ Editores, C.A.; 2009, p. 29–46.

[14] Fernández E. Low-rank radiosity. In: Rodríguez O, Serón F, Joan-Arinyo R, J. Madeiras J. Rodríguez EC, editors. Proceedings of the IV Iberoamerican Symposium in Computer Graphics. Sociedad Venezolana de Computación Gráfica; DJ Editores, C.A.; 2009, p. 55–62.

[15] Kontkanen J, Turquin E, Holzschuch N, Sillion F. Wavelet radiance transport for interactive indirect lighting. In: Heidrich W, Akenine-Möller T, editors. Rendering Techniques 2006 (Eurographics Symposium on Rendering). Eurographics; 2006, p. 161–71.

[16] Goldfeld SM, Quandt RE, Trotter HF. Maximization by Quadratic Hill-Climbing; vol. 34. The Econometric Society; 1966.

[17] Russell SJ, Norvig P. Artificial Intelligence: A Modern Approach. Pearson Education; 2 ed.; 2003.

[18] Kirkpatrick S, Gelatt CD, Vecchi MP. Optimization by simulated annealing. Science 1983;220(4598):671–80.

[19] Cassol F, Schneider PS, França FH, Neto AJS. Multi-objective optimization as a new approach to illumination design of interior spaces. Building and Environment 2011;46(2):331 –8.

[20] Schneider PS, Mossi AC, Franca FHR, de Sousa FL, da Silva Neto AJ. Application of inverse analysis to illumination design. Inverse Problems in Science and Engineering 2009;17(6):737–53.

[21] Russell S. The Architecture of Light: Architectural Lighting Design, Concepts and Techniques: a Textbook of Procedures and Practices for the Architect, Interior Designer and Lighting Designer. Conceptnine; 2008.

[22] Luenberger D, Ye Y. Linear and Nonlinear Programming. International Series in Operations Research & Management Science; Springer; 2008.

[23] Golub GH, Van Loan CF. Matrix computations (3rd ed.). Baltimore, MD, USA: Johns Hopkins University Press; 1996.

[24] Fernández E, Ezzatti P, Nesmachnow S, Besuievsky G. Low-rank radiosity using sparse matrices. In: Proceedings of GRAPP2012. 2012, p. 260–7.

[25] Cohen M, Wallace J, Hanrahan P. Radiosity and realistic image synthesis. San Diego, CA, USA: Academic Press Professional, Inc.; 1993.

[26] Lehtinen J, Zwicker M, Turquin E, Kontkanen J, Durand F, Sillion FX, et al. A meshless hierarchical representation for light transport. In: ACM SIGGRAPH 2008. New York, NY, USA: ACM; 2008, p. 1–9.

[27] Deb K. Multi-Objective Optimization using Evolutionary Algorithms. Wiley-Interscience Series in Systems and Optimization; John Wiley & Sons, Chichester; 2001.

[28] Coello CC, Lamont G, van Veldhuizen D. Evolutionary Algorithms for Solving Multi-Objective Problems. Genetic and Evolutionary Computation; Berlin, Heidelberg: Springer; 2nd ed.; 2007.

[29] Talbi EG. Metaheuristics: From Design to Implementation. Wiley Publishing; 2009.